Available online at www.sciencedirect.com
ScienceDirect
Trans. Nonferrous Met. Soc. China 23(2013) 2657−2665
Transactions of Nonferrous Metals Society of China
www.tnmsc.cn

Adsorption behavior and adsorption mechanism of Cu(II) ions on amino-functionalized magnetic nanoparticles

Hui LI[1], De-li XIAO[1], Hua HE[1,2], Rui LIN[3], Peng-li ZUO[1]

1. Department of Analytical Chemistry, China Pharmaceutical University, Nanjing 210009, China;
2. Key Laboratory of Drug Quality Control and Pharmacovigilance of Ministry of Education, China Pharmaceutical University, Nanjing 210009, China;
3. Yancheng Health Vocational and Technical College, Yancheng 224005, China

Received 23 August 2012; accepted 3 December 2012

Abstract: Amino-functionalized magnetic nanoparticle (NH_2−MNP) were prepared by a sol−gel approach. The adsorption behavior of Cu(II) ions on NH_2−MNP was discussed systematically by batch experiments. The effects of initial Cu(II) ions concentration, time, pH and temperature were investigated. In kinetic studies, the pseudo-second-order model was successfully employed, and the pseudo-first-order model substantiated that Cu(II) adsorption on NH_2−MNP was a diffusion-based process. Langmuir model and Dubinin−Radushkevich model (R^2>0.99) were more corresponded with the adsorption isotherm data of Cu(II) ions than Freundlich model. The adsorption capacity was increased with the increment of temperature and pH. NH_2−MNP remains excellent Cu(II) recoveries after reusing five adsorption and desorption cycles, making NH_2−MNP a promising candidate for repetitively removing heavy metal ions from environmental water samples. According to the results obtained from adsorption activation energy and thermodynamic studies, it can be inferred that the main adsorption mechanism between absorbent and Cu(II) ions is ion exchange–surface complexation.

Key words: amino-functionalized magnetic nanoparticles; Cu(II) ions; adsorption; ion exchange−surface complexation

1 Introduction

Heavy metal ions in the environment arise from both natural and industrial emissions. They not only can be non-degradable, but also will be accumulated in animals, plants and human body, causing serious disorders. Therefore, the disposal of heavy metal ions has been listed as a priority and the standards of emissions have become increasingly strict. In the past few decades, many conventional methods have been developed to remove heavy metal ions, including oxidation, reduction, precipitation, membrane filtration, ion exchange and adsorption [1−7]. Nowadays, adsorption has become one of the most promising methods for removing metal ions from wastewater due to their regeneration, high efficiency and economy.

There are two major kinds of mechanisms between adsorbents and adsorbates (organic and inorganic substances), i.e. physical adsorption [8] or chemical adsorption [9]. Copper ions which exist as cations in aqueous solution at low pH could be removed via surface complexation [10] or electrostatic attraction [11]. Thus, one of the effective approaches to remove the copper ions is to chemically graft various functional groups, including carboxyl, hydroxyl, phosphate, mercapto, amide and amino groups onto the surface of adsorbent [8,12−14]. YANTASEE et al [15] reported that amino groups which combine with ions through coordination interaction, normally have stronger selectivity to Cu^{2+} than that to Pb^{2+}, Ni^{2+} or Cd^{2+}.

Recently, magnetic separation technology as a kind of high efficient, rapid and economic separation method, has been widely developed in mining, microbiology, diagnostics and environment protection [16−18]. In this work, based on the previous studies [10,19], amino-functionalized magnetic nanoparticles (NH_2−MNP) were prepared by a sol−gel approach and the

Foundation item: Project (CXZZ11-0812) supported by Graduate Students Innovative Projects of Jiangsu Province, China; Project (J20122288) supported by Guizhou Provincial Natural Science Foundation of China; Project (Y4110235) supported by Zhejiang Provincial Natural Science Foundation of China; Project (JKY2011008) supported by Fundamental Research Funds for the Central Universities, China
Corresponding author: Hua HE; Tel: +86-25-83271508; E-mail: dochehua@163.com
DOI: 10.1016/S1003-6326(13)62782-X

adsorption behavior and mechanism of copper ions were investigated.

2 Experimental

2.1 Materials

Ferric chloride hexahydrate was obtained from Yufeng Chemical Reagents Company (Changsha, China). Tetraethyl orthosilicate (TEOS) and 3-aminopropyltrieth-oxysilan (DB-550) were purchased from Aladdin Chemical Reagents Company (Shanghai, China) and Diomand New Materials of Chemical Inc. (Hubei, China), respectively. Sodium diethyldithiocarbamate (DDTC), as the chelating agent, was gained from Tingxin Chemical Reagents Company (Shanghai, China). Pentahydrate copper sulfate ($CuSO_4·5H_2O$) was used to get Cu(II) stock solutions. All chemicals used in the experiments were purchased from being analytically pure. The whole process was conducted in deionized (DI) water.

2.2 Synthesis of NH_2−MNP

The preparation of magnetic nanoparticles (MNP) was based on our previous work [20]. A sol−gel approach was taken up according to the work by LU et al [21] to prepare the silica coated magnetic nanoparticles (SiO_2−MNP). 1.0 g MNP was diluted with the mixture of 8 mL deionized water and 40 mL ethanol. Under continuous mechanical stirring, 0.5 mL ammonia solution (30%, m/v) and 0.5 mL TEOS were consecutively added to the mixture. The reaction was allowed to proceed at room temperature (25 °C) for 3 h under continuous stirring. Then the obtained SiO_2−MNP was used for preparing NH_2−MNP. The procedure was the same as that of preparing SiO_2−MNP except using 0.9 mL DB−550 instead of 0.5 mL TEOS. The obtained NH_2−MNP was washed several times with ethanol and water, and then dried in vacuum at 65 °C for 10 h.

2.3 Determination of Cu(II)

A stable Cu(II)−DDTC complex [22] with low water-solubility, can be adequately extracted from aqueous medium with non-polar organic solvents, e.g. tetrachloromethane [23]. However, spectrophotometric analysis of Cu(II)−DDTC complex without the use of harmful substances is advocated and has successfully been conducted by many researchers in aqueous medium [24−26]. The reaction of DDTC and heavy metal ions was conducted in the molar ratio of 2:1 [27,28].

In this work, the exact amount of Cu(II) solution, 2.00 mL PEG−1500 solution (2%, m/v), DI water were moved into 10 mL volumetric flask, and HCl or NaOH was used to adjust pH to 8.0, which ensures the stability of Cu(II)−DDTC complex. Then, 2.00 mL DDTC solution (2%, m/v) was added to form complex with copper ions. The complex was placed for 5 min and measured the absorbance at about 454 nm by UV1800 UV−Vis spectrophotometer (Shimadzu Corporation, Japan). The blank absorbance of reagents was corrected before each determination.

In the range of 2.0−8.0 mg/L, the linear equation of standard curve is A=0.0101ρ−0.0091 (R^2=0.9999, n=6), where A is the absorbance, and ρ is the concentration of Cu(II). The relatively standard deviations (RSD) of intra-day precisions taken at the concentration of 3.5, 5.0, 6.5 mg/L are all less than 1%, which are negligible.

2.4 Batch adsorption experiment

The adsorption behavior of Cu(II) on adsorbents was investigated by batch technique. Before being used all the apparatus were immersed in the concentrated nitric acid for 24 h to minimize container adsorption. The absorbents suspensions were added into Cu(II) solutions. To investigate the effect of pH and temperature, 25 mL of 300 μg Cu(II) with pH ranging from 1.0 to 6.0 (or with temperature ranging from 293−353 K) was mixed with 2.5 mg NH_2−MNP for 24 h to reach equilibrium. For the adsorption kinetic studies, 15 mg NH_2−MNP was added into 150 mL of 3000 μg Cu(II). Adsorption isotherm was obtained by varying the initial Cu(II) concentration from 25 to 450 μg/25 mL at 298 K and pH 6.0. To conduct the desorption study, 2.5 mg loaded adsorbents were dispersed into 20 mL DI water with pH changing from 6.0 to 1.0. The desorption dynamic process was studied at the optimized pH 1.0. The suspension of loaded NH_2−MNP (1 mg) was dispersed to 200 mL nitric acid solution (pH=1.0).

The amount of adsorbed Cu(II) is calculated by

$$q_t = \frac{(\rho_0 - \rho_t)V}{m} \quad (1)$$

where q_t is the amount of Cu(II) adsorbed on absorbents; ρ_0 and ρ_t are the concentrations of Cu(II) at the initial and time t; respectively; V is the solution volume; m is the mass of adsorbents.

3 Results and discussion

3.1 Dispersion stability, magnetic performance and acid fastness, alkali resistivity of NH_2−MNP

The surface grafting of amino groups, the hydrophilic groups, can improve the solubility or dispersibility of adsorbents in DI water [29,30]. Figure 1(a) shows that NH_2−MNP can be dispersed well in DI water.

Being easily separated from the medium within a few seconds by adding an external magnetic field makes magnetic materials a promising candidate. In Fig. 1(b),

NH_2−MNP in DI water can be aptly separated in a few seconds with the transparent supernatant.

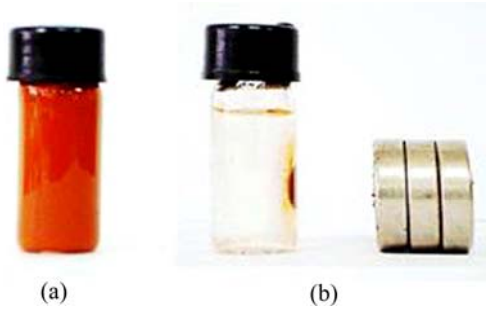

Fig. 1 Dispersion state (a) and magnetic performance (b) of NH_2−MNP in DI water

To determine the acid fastness and alkali resistivity of the adsorbents, NH_2−MNP was dispersed into solutions with pH ranging from 1.0 to 14.0. The pellucid supernatants were obtained, indicating that NH_2−MNP were stable in different pH solutions.

3.2 Characterization of NH_2−MNP

TEM by H−800, Hitachi Corporation, Japan shown in Fig. 2(a) and SEM by S−3000, Hitachi Corporation, Japan shown in Fig. 2(b) present the core-shell structure and the morphology of NH_2−MNP, respectively. Figure 2(a) shows that the polymer has a coating thickness of about 20 nm, which can be easily controlled [21] in the range of 2−100 nm by controlling the concentration of TEOS and DB−550 precursors. Figure 2(b) shows approximate round sphere and good dispersity of NH_2−MNP.

Figure 2(c) shows the surface groups on NH_2−MNP analyzed with 8400s FTIR spectrometer (Shimadzu Corporation, Japan). The doublet at 3479 cm^{-1} and 3410 cm^{-1} stands for N—H stretch, indicating the successful graft of amino groups. Peaks at 1637 cm^{-1} and 1068 cm^{-1} are evident for N — H bend and C — N stretch, respectively. Peak of Fe_3O_4 appears at 625 cm^{-1}.

3.3 Adsorption isotherms

To study the adsorption capacity of Cu(II) ions on NH_2−MNP, Langmuir, Freundlich and Dubinin−Radushkevich (D−R) isothermal models were employed to evaluate the obtained data shown in Fig. 3.

The Langmuir model is suitable for monolayer adsorption on a surface, and expressed as

$$\frac{\rho_e}{q_e}=\frac{\rho_e}{q_0}+\frac{1}{q_0K_L} \quad (2)$$

where q_e is the adsorbed Cu(II) concentration at the balance; ρ_e is Cu(II) concentration in solution at the balance; q_0 is the maximum adsorption capacity; K_L represents the adsorption energy.

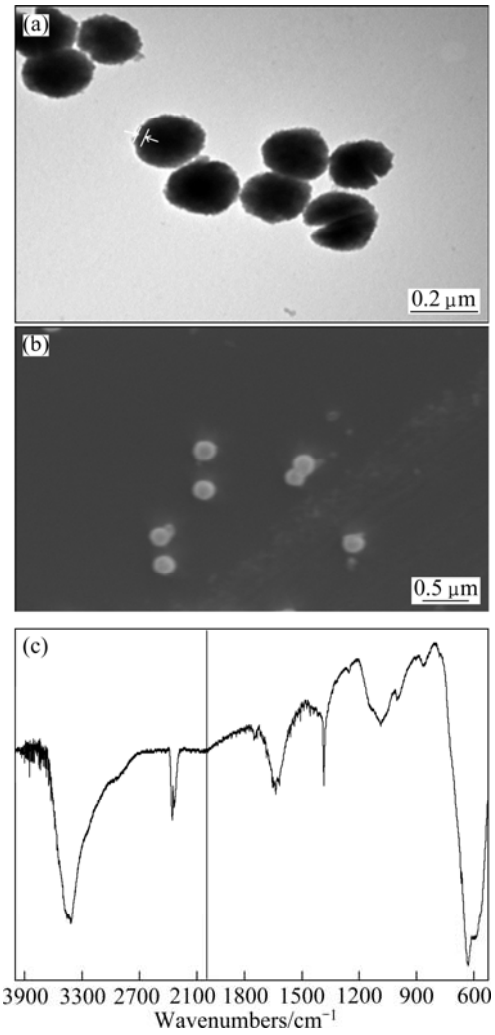

Fig. 2 TEM image (a), SEM image (b) and FTIR spectrum (c) of NH_2−MNP

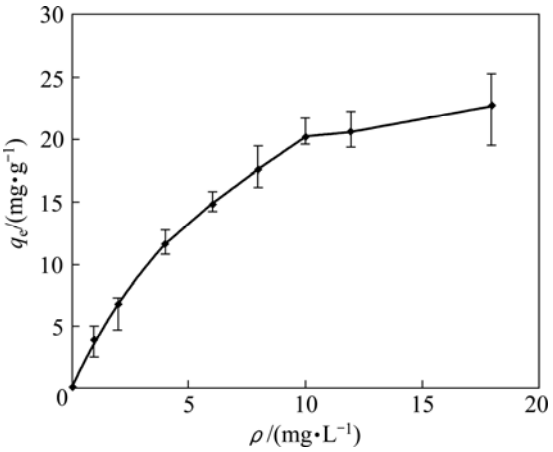

Fig. 3 Adsorption isotherm of Cu(II) ions on NH_2−MNP (V=25.0 mL, m(NH_2−MNP)= 2.5 mg, θ= 25 °C, pH= 6.0, t=240 min)

Freundlich model is applied on the basis of premising that stronger binding sites are occupied first. The Freundlich equation can be expressed as

$$\lg q_e = \lg K_F + \frac{1}{n}\lg \rho_e \quad (3)$$

where K_F is related to the adsorption capacity. The bigger the K_F is, the greater the adsorption capacity is. In addition, the values of n, which indicate the adsorption driving force, in the range 1–10, represent good tendency of adsorption [31].

The D−R model can be suitable for depicting the adsorption behavior on both homogeneous and inheterogeneous surfaces at low concentrations [32]. The D−R equation can be expressed in the linear form as

$$\ln q_e = \ln q_0 - \beta\varepsilon^2 \quad (4)$$

$$\varepsilon = RT\ln\left(1+\frac{1}{\rho_e}\right) \quad (5)$$

where β is the adsorption free energy; R is the gas constant; T is the thermodynamic temperature; ε is the Polanyi potential. Adsorption activation energy (E_a) is representative of the adsorption mechanism which can be expressed as

$$E_a = (2\beta)^{-1/2} \quad (6)$$

where E_a in the range of 8−16 kJ/mol is designated for ion-exchange mechanism [33].

Sorption isotherms of Cu(II) ions on NH_2−MNP simulated by the three models are shown in Fig. 4. All the correlation coefficient and constants are listed in Table 1. Obviously, Langmuir model and D−R model (R^2>0.98) give a better fit than Freundlich model. The exponent n of 1.79 is in the range of 1−10, indicating a favorable adsorption. E_a calculated from Eq. (6) is 14.75 kJ/mol, showing that the adsorption mechanism is ion exchange.

3.4 Adsorption kinetics

The adsorption of Cu(II) ions onto NH_2−MNP at optimized condition is shown in Fig. 5(a). The initial stage of adsorption has a relatively rapid adsorption rate, then Cu(II) loading rate on NH_2−MNP slowly decreases and finally reaches balance at about 90 min.

The pseudo-first-order model and the pseudo-second-order model were adopted to analyze the adsorption kinetics of Cu(II) on NH_2−MNP. The linear forms of the models are as follows:

$$\lg(q_e - q_t) = \lg q_e - \frac{k_1}{2.303}t \quad (7)$$

$$\frac{t}{q_t} = \frac{1}{k_2 q_e^2} + \frac{1}{q_e}t \quad (8)$$

where k_1 and k_2 are the adsorption rate constants of first- and second-order kinetic models, respectively; q_e and q_t

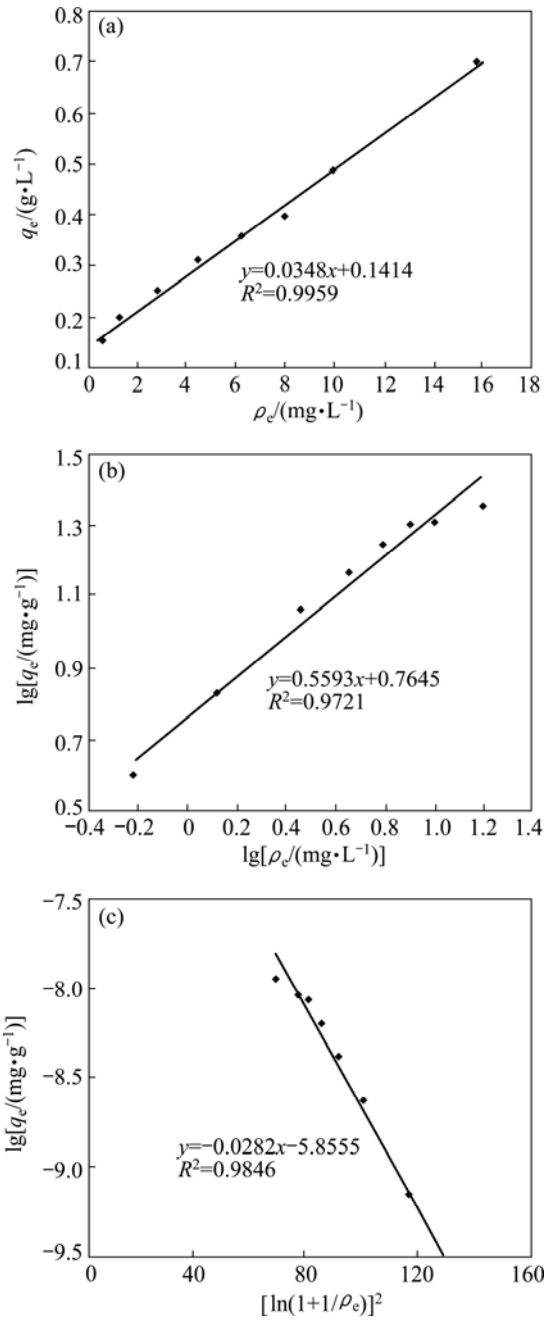

Fig. 4 Langmuir (a), Freundlich (b) and D−R (c) models for Cu(II) adsorption on NH_2−MNP (V= 25.0 mL, m(NH_2−MNP)= 2.5 mg, θ=25 °C, pH=6.0, t= 240 min)

Table 1 Freundili, Langmuir and D−R model correlation coefficients and constants for adsorption of Cu(II) on absorbents at 25 °C

Model	Parameter		
Freundlich	K_F/(mg^{1-n} L^n·g^{-1})	n	R^2
	5.81	1.79	0.972
Langmuir	q_0/(mg·g^{-1})	K_L/(L·mg^{-1})	R^2
	28.7	0.25	0.996
D−R	q_0/(mg·g^{-1})	β/10^{-3} mol^2·kJ^2)	R^2
	183.3	2.30	0.985

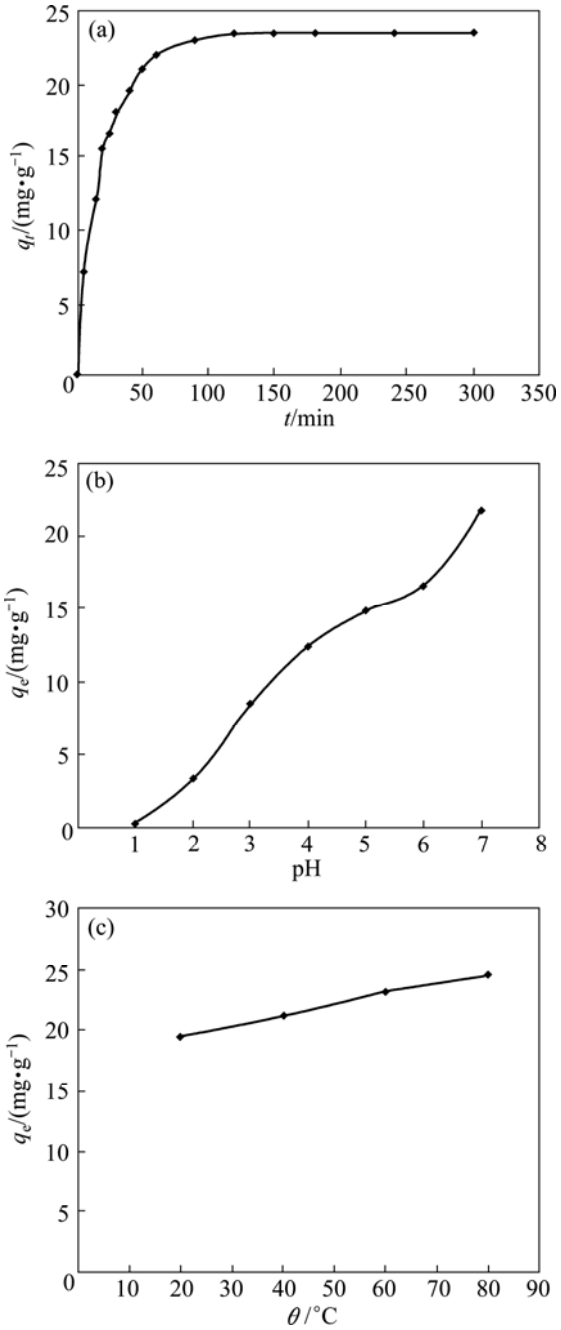

Fig. 5 Effect of time (a), pH (b) and temperature (c) on adsorption capacity of Cu(II) on NH_2−MNP

represent the equilibrium adsorption capacity and adsorption uptake at time t.

A plot (Fig. 6(a)) of $\lg(q_e-q_t)$ versus t according to the pseudo-first-order kinetic model gives a straight line at the initial 60 min. However, the pseudo-second-order kinetic model (Fig. 6(b)) is suitable for the whole adsorption process. The adsorption rate constants (k_1 and k_2) calculated from the slope and the intercept of each linear plot are listed in Table 2. The consistency of the experimental q_e (24.0 mg/g) with q_e (24.6 mg/g) calculated from the pseudo-second-order kinetic model indicates that the adsorption of Cu(II) onto NH_2−MNP at

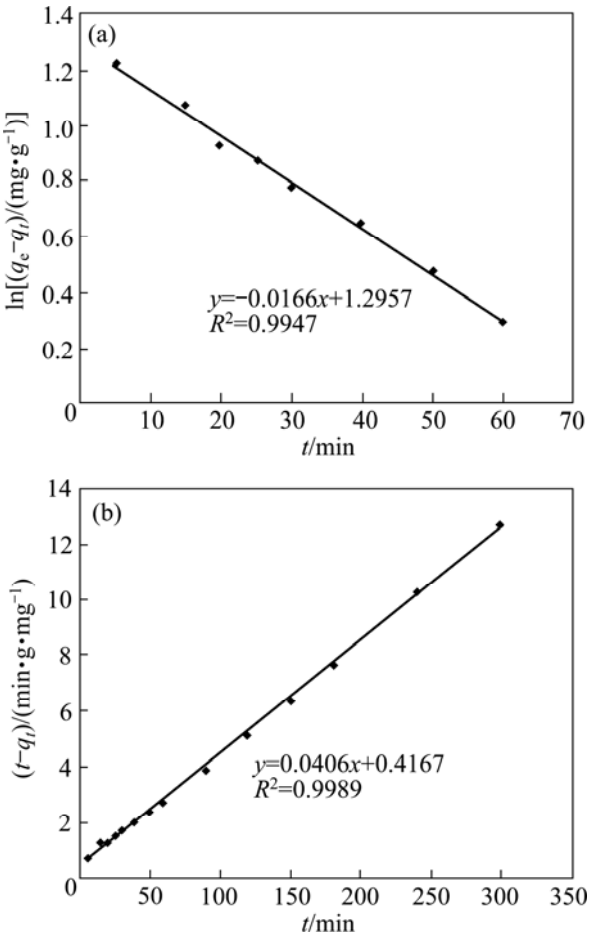

Fig. 6 Pseudo-first-order (a) and pseudo-second-order (b) kinetic models for adsorption of Cu(II) onto NH_2−MNP

Table 2 Parameters of pseudo-first-order and pseudo-second-order kinetic models for adsorption of Cu(II) onto NH_2−MNP

Pseudo-first-order kinetic model			Pseudo-second-order kinetic model		
q_e/(mg·g^{-1})	k_1/min^{-1}	R^2	q_e/(mg·g^{-1})	k_2/(g·mg^{-1}·min^{-1})	R^2
19.76	0.0382	0.995	24.6	3.96×10^{-3}	0.999

initial concentration of 20 mg/L is controlled by chemical adsorption [34]. The correspondence with the pseudo-first-order kinetic model substantiates that Cu(II) adsorption onto NH_2−MNP is a diffusion-based process [35].

The intra-particle diffusion equation is given as

$$q_t = k_p t^{1/2} + C \quad (9)$$

where k_p is the intra-particle rate constant; C is a constant related to the thickness of the boundary layer.

Adsorption process essentially can be divided into three steps. The first step is mass transfer through water film to adsorbent surface (film diffusion); the second one

is a pore diffusion of adsorbates or a solid surface diffusion; the third one is occupation at a site on the surface through physical or chemical adsorption. It is obvious in Fig. 7 that plots give multi-linear plots over the whole time range. The slope of the linear portion indicates the rate of the adsorption. The first stage is an external diffusion to the exterior surface of adsorbent which is the fastest; the second linear portion which takes the second place is a gradual adsorption. Due to decreasing Cu^{2+} concentration in solutions and available adsorption sites, the third portion, which has the lowest rate, is approaching equilibrium. In sum, the intra-particle diffusion is the rate-controlling step.

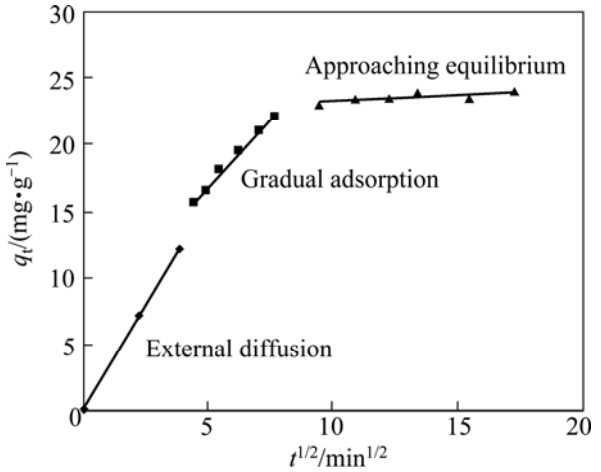

Fig. 7 Intra-particle diffusion model for adsorption of Cu(II) onto NH_2−MNP

3.5 Effect of pH on adsorption

There are mainly four forms of Cu(II) ions in DI water i.e., Cu^{2+}, $Cu(OH)^+$, $Cu(OH)_2^0$ and $Cu(OH)_3^-$. At pH>7, copper ions may start to precipitate at the initial Cu(II) concentration of 20 mg/L [36]. Thus, the optimized pH of the experimental system should be smaller than 7.0 to prevent Cu(II) from precipitation.

The amount of Cu(II) loaded on NH_2−MNP with different pH is shown in Fig. 5(b). The adsorption capacity of Cu(II) on NH_2−MNP increased from 1.76 mg/g to 22.4 mg/g with the increment of pH from 1.0 to 6.0, indicating that the adsorption capacity of Cu(II) to NH_2−MNP was highly pH dependent.

3.6 Adsorption thermodynamics

The results of the thermodynamics experiment are shown in Fig. 5(c). The adsorption capacity of Cu(II) on NH_2−MNP increased from 19.2 mg/g to 24.5 mg/g with the increment of temperature from 293 (20 °C) to 353 K (60 °C), suggesting that adsorption of Cu(II) on to NH_2−MNP is an endothermic process.

The data shown in Fig. 5(c) were analyzed by the following equations [37]:

$$K_D = \frac{\rho_0 - \rho_e}{\rho_e}\frac{V}{m} \tag{10}$$

$$\ln K_D = -\frac{\Delta H^\Theta}{RT} + \frac{\Delta S^\Theta}{R} \tag{11}$$

where K_D is the distribution coefficient; ρ_0 is the initial concentration of Cu(II); ρ_e is the equilibrium concentration of Cu(II); V is the solution volume; m is the mass of NH_2−MNP; ΔH^Θ and ΔS^Θ are standard enthalpy change and standard entropy change, respectively.

Gibbs free energy changes (ΔG^Θ) can be calculated from

$$\Delta G^\Theta = \Delta H^\Theta - T\Delta S^\Theta \tag{12}$$

Relevant parameters calculated from Eqs. (11) and (12) are given in Table 3.

Table 3 Thermodynamic parameters for Cu(II) adsorption on NH_2−MNP (ρ[Cu(II)]$_{initial}$=12 μg/mL, V=25.0 mL, m(NH_2−MNP)=2.5 mg, pH=6.0, t= 240 min)

Temperature/K	ΔH^Θ/(kJ·mol^{-1})	ΔS^Θ/(J·mol^{-1}K^{-1})	ΔG^Θ/(kJ·mol^{-1})
293	4.19	19.77	−1.60
313			−1.99
333			−2.39
353			−2.78

The positive value of ΔH^Θ represents an endothermic adsorption process, indicating that the adsorption mechanism is chemical adsorption. ΔG^Θ is negative as expected for a spontaneous process under our experimental conditions. The decrease of ΔG^Θ with the increase of temperature indicates more efficient adsorption at higher temperatures. The positive values of entropy change (ΔS^Θ) reflect the affinity of NH_2−MNP towards Cu(II) ions in aqueous solutions. Thus, temperature is an important parameter for the adsorption process.

3.7 Adsorption mechanism

Chemical adsorption, produced by chemical bonds force, bears the traits of selectivity, irreversibility and is endothermic process. According to the results of thermodynamics, the adsorption mechanism of Cu(II) on NH_2−MNP is chemical adsorption (surface complexation); according to the result obtained from E_a, the adsorption mechanism of Cu(II) on NH_2−MNP is ion exchange. Combining the two results, it is possible to presume that the adsorption mechanism of Cu(II) on NH_2−MNP is more likely to be a combined ion exchange−surface complexation [38]. Thus, the

adsorption mechanism at optimized pH is a rapid ion exchange of amino hydrolysis through hydrogen bond between amino and hydroxyl groups, and slow chemisorption or/and an surfacing complexation. Also, the hydrolyzed amino can react with copper ions through electrostatic attraction. The interaction between the adsorbents and Cu(II) may be described by Eqs.(13)−(17).

$$-NH_2 + H^+ \rightleftharpoons -NH_3^+ \quad (13)$$

$$-NH_2 + Cu^{2+} \rightleftharpoons -NH_2Cu^{2+} \quad (14)$$

$$-NH_2 + Cu^{2+} + H_2O \rightleftharpoons -NH_2Cu(OH)^+ + H^+ \quad (15)$$

$$-NH_2 + H_2O \rightleftharpoons -NH_2OH^- + H^+ \quad (16)$$

$$-NH_2OH^- + Cu^{2+}(CuOH^+) \rightleftharpoons -NH_2OH^-\cdots Cu^{2+}(-NH_2OH^-\cdots CuOH^+) \quad (17)$$

Equation (13) indicates protonation/deprotonation reaction of the amino on the surface of NH_2−MNP in the solution. Equations (14) and (15) show the formation of surface complexes of $Cu^{2+}(CuOH^+)$ with the amino via coordination interactions. At lower pH, electrostatic repulsion between NH^{3+} and Cu^{2+} can be caused by amino protonation, suggesting that the regeneration of unloaded NH_2−MNP can be easily achieved by subjecting the Cu^{2+} loading NH_2−MNP to an acidic solution. With the increase of pH, in regard to Eqs. (16) and (17), amino groups have ion exchange with hydroxyl groups from the solution through hydrogen bond, reacting with $Cu^{2+}(CuOH^+)$ through electrostatic attraction or/and surface complexation.

In sum, the main contributions are surface complexation and electrostatic attraction between amino and $Cu^{2+}(CuOH^+)$. And surface complexation, which is chemisorption, takes the dominant place of the two mechanisms. The possible adsorption reaction between NH_2−MNP and copper ions can be depicted as Fig. 8.

3.8 Desorption of Cu(II)

A promising adsorbent should not only possess a higher adsorption capability, but also bear an ability of repeated usage, which will remarkably save the overall cost in the industrial production. K_D obtained from Eq. (10) can reflect the stability of a complex at a particular pH. Higher K_D represents more stable complex. K_D of Cu^{2+} at pH 2 or below, is negligible, suggesting that the regeneration of adsorbents can be easily performed by subjecting the loaded adsorbents to acid [15]. Thus, since NH_2−MNP can keep stable at pH 1.0−14.0, to elute Cu^{2+} from adsorbents. pH 1.0 was chosen as the eluting condition. Figure 9 shows Cu(II) desorption from NH_2−MNP as a function of time at pH 1.0. It can be seen that the desorption efficiency of Cu(II) reached 95% at pH 1.0. Cu(II) recovery on NH_2−MNP remained above 90.0% after a run of 5 adsorption/desorption cycles, making NH_2−MNP a promising candidate for repetitive adsorption/desorption of heavy metal ions in environmental water samples.

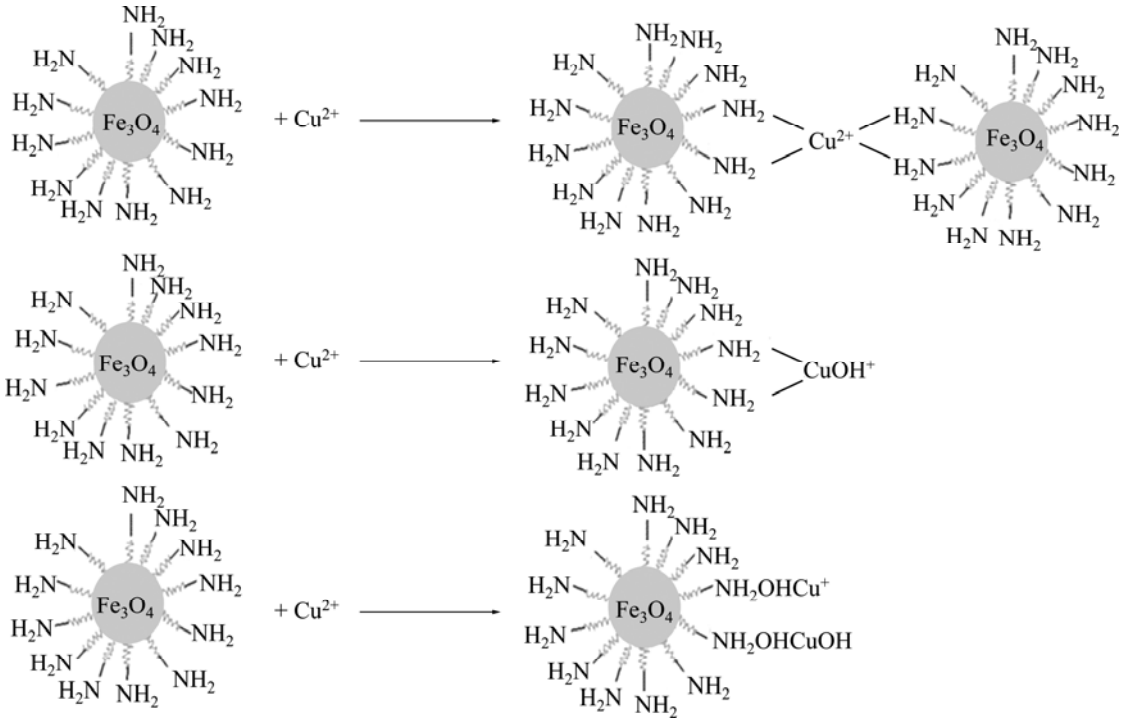

Fig. 8 Schematic diagram of major mechanism for adsorption of Cu(II) ions onto NH_2−MNP

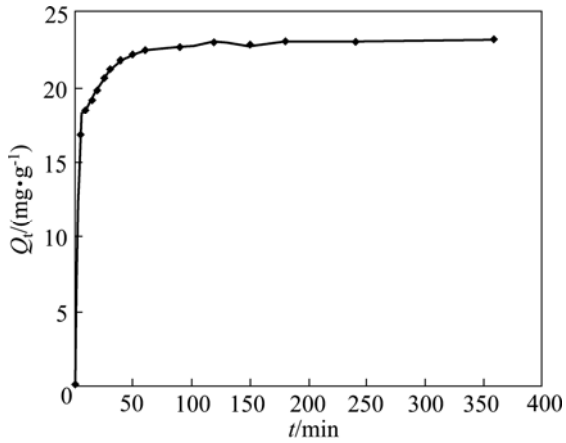

Fig. 9 Release kinetic curve of Cu(II) ions from NH_2−MNP at pH=1

4 Conclusions

NH_2−MNP was prepared by a sol−gel approach. The batch experiments show that NH_2−MNP bears high adsorption capacity and convenience of separation. The easy adsorption/desorption of copper ions makes NH_2−MNP a potential adsorbent for fast extraction of heavy metal ions from environmental samples. The main adsorption mechanism of copper ions onto the surface of NH_2−MNP is surface complexation and electrostatic attraction between amino groups and Cu^{2+}($CuOH^+$). And surface complexation, which is chemisorption, takes the dominant place of the two mechanisms. These findings will deepen the cognition to the heavy metal adsorption mechanism which may bring some further understanding design and preparation of nano-magnetic adsorbents.

References

[1] KUMASHIRO R, KURODA Y, NAGAO M. New analysis of oxidation state and coordination environment of copper ion-exchanged in ZSM-5 zeolite [J]. Journal of Physical Chemistry B, 1999, 103: 89−96.

[2] LIN S W, NAVARRO R M F. An innovative method for removing Hg^{2+} and Pb^{2+} in ppm concentrations from aqueous media [J]. Chemosphere, 1999, 39: 1809−1817.

[3] ESALAH J, HUSEIN M M. Removal of heavy metals from aqueous solutions by precipitation-filtration using novel organo-phosphorus ligands [J]. Separation Science and Technology, 2008, 43: 3461−3475.

[4] SANG Y M, GU Q B, SUN T C, LI F S, LIANG C Z. Filtration by a novel nanofiber membrane and alumina adsorption to remove copper(II) from groundwater [J]. Journal of Hazardous Materials, 2008, 153: 860−866.

[5] PETRUZZELLI D, PAGANO M, TIRAVANTI G, PASSINO R. Lead removal and recovery from battery wastewaters by natural zeolite clinoptilolite [J]. Solvent Extraction and Ion Exchange, 1999, 17: 677−694.

[6] DYER J A, TRIVEDI P, SCRIVNER N C, SPARKS D L. Lead sorption onto ferrihydrite. 2. Surface complexation modeling [J]. Environmental Science and Technology, 2003, 37: 915−922.

[7] OLIVEIRA L C A, RIOS R V R A, FABRIS J D, GARG V, SAPAG K, LAGO R M. Activated carbon/iron oxide magnetic composites for the adsorption of contaminants in water [J]. Carbon, 2002, 40: 2177−2183.

[8] CHEN Z, PIERRE D, HE H, TAN S H, PHAM-HUY C, HONG H, HUANG J L. Adsorption behavior of epirubicin hydrochloride on carboxylated carbon nanotubes [J]. International Journal of Pharmaceutics, 2011, 405: 153−161.

[9] YAMADA K, AKIBA Y, SHIBUYA T, KASHIWADA A, MATSUDA K, HIRATA M. Water purification through bioconversion of phenol compounds by tyrosinase and chemical adsorption by chitosan beads [J]. Biotechnology Progress, 2005, 21: 823−829.

[10] SHEN H Y, PAN S D, ZHANG Y, HUANG X L, GONG H X. A new insight on the adsorption mechanism of amino-functionalized nano-Fe_3O_4 magnetic polymers in Cu(II), Cr(VI) co-existing water system [J]. Chemical Engineering Journal, 2012, 183: 180−191.

[11] EL-SHEIKH A H. Effect of oxidation of activated carbon on its enrichment efficiency of metal ions: Comparison with oxidized and non-oxidized multi-walled carbon nanotubes [J]. Talanta, 2008, 75: 127−134.

[12] PARK J J, PARK D M, YOUK J H, YU W R, LEE J Y. Functionalization of multi-walled carbon nanotubes by free radical graft polymerization initiated from photoinduced surface groups [J]. Carbon, 2010, 48: 2899−2905.

[13] AGUADO J, ARSUAGA J M, ARENCIBIA A, LINDO M, GASCON V. Aqueous heavy metals removal by adsorption on amine-functionalized mesoporous silica [J]. Journal of Hazardous Materials, 2009, 163: 213−221.

[14] PEREZ-QUINTANILLA D, HIERRO I D, CARRILLO-HERMOSILLA F, FAJARDO M, SIERRA I. Adsorption of mercury ions by mercapto-functionalized amorphous silica [J]. Analytical and Bioanalytical Chemistry, 2006, 384: 827−838.

[15] YANTASEE W, LIN Y H, FRYXELL G E, ALFORD K L, BUSCHE B J, JOHNSON C D. Selective removal of copper(II) from aqueous solutions using fine-grained activated carbon functionalized with amine [J]. Industrial and Engineering Chemistry Research, 2004, 43: 2759−2764.

[16] NGOMSIK A F, BEE A, DRAYE M, COTE G, CABUIL V. Magnetic nano- and micro-particles for metal removal and environmental applications: A review [J]. Comptes Rendus Chimie, 2005, 8: 963−970.

[17] ZHANG Y S, ZHU J Y, ZHANG L, ZHANG Z M, XU M, ZHAO M J. Synthesis of EDTAD-modified magnetic baker's yeast biomass for Pb^{2+} and Cd^{2+} adsorption [J]. Desalination, 2011, 278: 42−49.

[18] XU M, ZHANG Y S, ZHANG Z M, SHEN Y O, ZHAO M J, PAN G T. Study on the adsorption of Ca^{2+}, Cd^{2+} and Pb^{2+} by magnetic Fe_3O_4 yeast treated with EDTA dianhydride [J]. Chemical Engineering Journal, 2011, 168: 737−745.

[19] HUANG S H, CHEN D H. Rapid removal of heavy metal cations and anions from aqueous solutions by an amino-functionalized magnetic nano-adsorbent [J]. Journal of Hazardous Materials, 2009, 163: 174−179.

[20] XIAO D L, DRAMOU P, HE H, PHAM-HUY L A, LI H, YAO Y Y, PHAM-HUY C. Magnetic carbon nanotubes: Synthesis by a simple solvothermal process and application in magnetic targeted drug delivery system [J]. Journal of Nanoparticle Research, 2012, 14: 984−996.

[21] LU Y, YIN Y D, MAYERS B T, XIA Y N. Modifying the surface properties of superparamagnetic iron oxide nanoparticles through a sol−gel approach [J]. Nano Letters, 2002, 2: 183−186.

[22] SZPUNAR-LOBINSKA J, TROJANOWICZ M. Flow-injection extraction-spectrophoto-metric determination of copper with

dithiocarbamates [J]. Analytical Sciences, 1990, 6: 415−419.
[23] WEN X D, YANG Q L, YAN Z D, DENG Q W. Determination of cadmium and copper in water and food samples by dispersive liquid–liquid microextraction combined with UV-vis spectrophotometry [J]. Microchemical Journal, 2011, 97: 249−254.
[24] WANG P, SHI S J, ZHOU D. Sequential determination of nickel and copper in waste waters by reversed flow injection spectrophotometry [J]. Microchemical Journal, 1995, 52:146−154.
[25] STADEN J F V, BOTHA A. Spectrophotometric determination of Cu(II) with sequential injection analysis [J] Talanta, 1999, 49: 1099−1108.
[26] SANT'ANAA O D, JESUINOA L S, CASSELLA R J. Solid phase extraction of Cu(II) as diethyldithiocarbamate (DDTC) complex by polyurethane foam [J]. Journal of the Brazilian Chemical Society, 2003, 14: 728−733.
[27] WANG L Y, BAO J, WANG L, ZHANG F, LI Y D. One-pot synthesis and bioapplication of amine-functionalized magnetite nanoparticles and hollow nanospheres [J]. Chemistry-A European Journal, 2006, 12: 6341−6347.
[28] LIU P. Modifications of carbon nanotubes with polymers [J]. European Polymer Journal, 2005, 41: 2693−2703.
[29] HERNANDEZ M J M, ALVAREZ-COQUE M C G, RAMOS G R, FERNANDEZ C M. Catalytic-enthalpimetric determination of diethyldithiocarbamate (DDTC) and nickel(II) using the iodine-azide reaction [J]. Thermochimica Acta, 1985, 90: 277−285.
[30] CESUR H, AKSU Ç. Determination of cadmium and zinc in fertilizer samples by FAAS after solid-phase extraction with freshly precipitated manganese−diethyldithiocarbamate [J]. Analytical Sciences, 2006, 22: 727−730.
[31] SHAHWAN T, ERTEN H N. Temperature effects in barium sorption on natural kaolinite and chlorite-illite [J]. Journal of Radioanalytical and Nuclear Chemistry, 2004, 260: 43−48.
[32] VIJAYARAGHAVAN K, PADMESH T V N, PALANIVELU K, VELAN M. Biosorption of nickel(II) ions onto sargassum wightii: Application of two-parameter and three-parameter isotherm models [J]. Journal of Hazardous Materials, 2006, 133: 304−308.
[33] TOFIGHY M A, MOHAMMADI T. Adsorption of divalent heavy metal ions from water using carbon nanotube sheets [J]. Journal of Hazardous Materials, 2011, 185: 140−147.
[34] HAMDI M, DOGAN M, ALKAN M. Kinetic analysis of reactive blue 221 adsorption on kaolinite [J]. Desalination, 2010, 256: 154−165.
[35] ONYANGO M S, KOJIMA Y, AOYI O, BERNARDO E C, MATSUDA H. Adsorption equilibrium modeling and solution chemistry dependence of fluoride removal from water by trivalent-cation-exchanged zeolite F-9 [J]. Journal of Colloid and Interface Science, 2004, 279: 341−350.
[36] PAULSON A J, KESTER D R. Copper(II) ion hydrolysis in aqueous solution [J]. Journal of Solution Chemistry, 1980, 9: 269−277.
[37] ZHAO Y G, SHEN H Y, PAN S D, HU M Q, XIA Q H. Preparation and characterization of amino-functionalized nano-Fe_3O_4 magnetic polymer adsorbents for removal of chromium(VI) ions [J]. Journal of Materials Science, 2010, 45: 5291−5301.
[38] LYUBCHIK S I, LYUBCHIK A I, GALUSHKO O L, TIKHONOVA L P, VITAL J, FONSECA I M, LYUBCHIK S B. Kinetics and thermodynamics of the Cr(III) adsorption on the activated carbon from commingled wastes [J]. Colloids and Surfaces A, 2004, 242: 151−158.

铜离子在氨基化磁性纳米粒子上的吸附行为及吸附机理

李 卉[1]，肖得力[1]，何 华[1,2]，林 锐[3]，左朋礼[1]

1. 中国药科大学 分析化学教研室，南京 210009；
2. 中国药科大学 理学院 药物质量与安全预警教育部重点实验室，南京 210009；
3. 盐城卫生职业技术学院，盐城 224005

摘 要：通过溶胶−凝胶法制备氨基修饰的磁性纳米粒子。以紫外分光光度法为检测手段，采用静态批次实验研究不同实验参数(吸附时间、溶液 pH 和溶液温度)对铜离子吸附的影响。对铜离子的动力吸附学过程符合准二级动力学模型。准一级动力学模型证明其对铜离子的吸附是一个基于内部粒子扩散的过程。吸附等温线数据既符合 Langmuir 吸附等温模型又符合 Dubinin−Radushkevich 吸附等温式。随着溶液 pH 的增加和温度的升高，水中铜离子的去除效率也增加。另外，铜离子在低 pH 时可以很容易地从吸附材料上面洗脱下来，并且在材料重复使用 5 次之后，铜离子的回收率仍然保持在 90.0 %以上。根据吸附活化能和热力学实验结果，可以推断铜离子在吸附剂上的吸附机制是离子交换−表面络合。

关键词：氨基化磁性纳米粒子；铜离子；吸附；离子交换−表面络合

(Edited by Xiang-qun LI)